Fragmentation study of major spirosolane-type glycoalkaloids by Collision Induced Dissociation Linear Ion Trap (CID-LIT) and Infrared Multiphoton Dissociation Fourier Transform Ion Cyclotron Resonance (IRMPD-FT-ICR) mass spectrometry

Lelario F.[1*], Labella C.[1], Napolitano G. [1], Scrano L. [2], Bufo S.A. [1]

[1]*Department of Science, University of Basilicata, Potenza, Italy*

[2] *Department of European and Mediterranean Cultures, University of Basilicata, Matera, Italy*

* Authors for correspondence, e–mail: filomenalelario@hotmail.com

This article has been accepted for publication and undergone full peer review but has not been through the copyediting, typesetting, pagination and proofreading process which may lead to differences between this version and the Version of Record. Please cite this article as doi: 10.1002/rcm.7727

Abstract

RATIONALE: Glycoalkaloids play a key role in the plant protection system against phytopathogens including fungi, viruses, bacteria, insects and worms. They can be toxic to humans if consumed in high concentrations causing gastrointestinal disturbances.

METHODS: The structural characterization of the major spirosolane glycoalkaloids, solasonine, solamargine, α-tomatine and dehydrotomatine, were investigated by positive electrospray ionization (ESI) coupled with a hybrid linear ion trap (LIT) and Fourier-transform ion cyclotron resonance (FTICR) mass spectrometer. Tandem mass spectrometric analysis of spirosolane glycoalkaloids was performed by both collision-induced dissociation (CID) within the linear ion trap and infrared multiphoton dissociation (IRMPD) in conjunction with the FTICR cell.

RESULTS: Several common product ions were observed, generated by losses of sugar moiety or aglycon fragmentation in B- or E-rings, that can provide information on the accurate mass of aglycon and the primary sequence and branching of the oligosaccharide chains. Thanks to the multistage CID it was possible to understand the fragmentation pathways and thanks to high resolution of IRMPD-FTICR the elemental composition of product ions was obtained.

CONCLUSIONS: Because the investigated tandem mass spectra data were acquired with high mass accuracy, unambiguous interpretation and determination of the chemical composition for the majority of detected fragment ions were feasible. From these data, generalized fragmentation pathways were proposed, providing guidance for the characterization of unknown glycoalkaloids in plants.

KEYWORDS: IRMPD; FTICR MS; tandem MS; ion-cyclotron resonance; mass accuracy.

Introduction

Glycoalkaloids are a class of nitrogen-containing secondary metabolites of great structural variety that can be found in many plants of the Solanaceae family including eggplant (*Solanum Melongena)* and tomato (*Lycopersicon esclulentum*) [1, 2]. They play a key role in the plant protection system against phytopathogens including fungi, viruses, bacteria, insects, and worms and they may have both adverse and beneficial biological effects [3, 4]. Glycoalkaloids are toxic to humans if consumed in high concentrations causing gastrointestinal disturbances such as vomiting, diarrhoea and abdominal pain [5]. Owing to their widespread occurrence in edible plants in the human diet and the health-related properties that are attributed to glycoalkaloids, they have been subject to ever-increasing attention. Based on the structures of the aglycones, glycoalkaloids can be classified into two types: spirosolane and solanidane. Spirosolanes have an oxa-azaspirodecane alkaloid portion and solanidanes have fused indolizidine rings. The spirosolane-type GAs, solasonine and solamargine (Figs. 1a and 1b), are the major components of eggplant [6]. Their structures contain the same core aglycone structure, solasodine, and a three sugar unit (solatriose or chacotriose), that determines the structural difference [7]. Two other spirosolane-type GAs that play an important role in the metabolism of *Solanum* species are α-tomatine and dehydrotomatine (Figs. 1c and 1d) [8]. These compounds are most represented in tomato plants and only differ by the presence or absence of a double bond in the aglycone structure, tomatidine (α-tomatine) or tomatidenol (dehydrotomatine), to which a tetrasaccharide moiety lycotetraose is attached [9,10].

The presence of only small structural differences among various GAs requires the use of accurate and reproducible methods to identify and efficiently characterize them [11,12].

The identification of GAs has usually been made first by determination of their molecular weight and then confirmed by tandem MS fragmentation to obtain information on the nature of the aglycone unit and of the carbohydrate sequence [2,13]. For GAs structure investigation, mass spectrometry offers several possible fragmentation techniques [14,15]. ESI-FTICR MS provides a highly selective tool for the unambiguous identification of molecules, which can be extended to minor components without significant interferences of other compounds in the sample extracts [16]. Infrared multiphoton dissociation (IRMPD) is a tandem MS (MS/MS) method that has been successfully implemented in FT-ICR, time-of-flight, and quadrupole ion trap mass spectrometers [17,18].

In IRMPD energy from an infrared laser is transferred to trapped ions and used to fragment them. IRMPD fragmentation of GAs can be advantageous over collisional induced dissociation (CID), because the mechanism of IR activation is independent of the trapping voltage that can be set at a low value to retain the low *m/z* product ions, which are not typically observed by ion trap CID. Furthermore, because all ions are continuously irradiated during the activation period, IRMPD can also promote secondary dissociation of primary product ions and thus lead to the formation of a more diverse array of diagnostic ions than CID [19]. IRMPD-FT-ICR MS/MS thereby provides faster fragmentation analysis and higher resolution than multistage CID within a linear ion trap, leading to an unambiguous interpretation and determination of the chemical composition for the majority of detected product ions [20,21].

In this work, we have applied both dissociation techniques, CID and IRMPD, in a hybrid linear trap/7-T Fourier transform ion cyclotron resonance mass spectrometer, for the investigation of spirosolane-type glycoalkaloids (SGAs) solamargine, solasonine, α-tomatine and dehydrotomatine fragmentation pathways by direct-infusion MS experiments. The two types of spectra at low and high resolution obtained with the same instrument thus offer

complementary structural information, which can be used in the identification of known and unknown GAs in plants. IRMPD provided abundant accurate product ions and CID aided the elucidation of the mass fragmentation pathways.

Materials and Methods

Chemicals

Acetonitrile (ACN), LC-MS grade, and formic acid (99%) were from Carlo Erba (Milan, Italy). Ultrapure water was produced using a Milli-Q system from Millipore (Billerica, MA, USA). Pure solamargine (97.5%) and solasonine (98.3%) were purchased from Glycomix (Reading, UK), while α-tomatine, containing dehydrotomatine as impurity (tomatine:dehydrotomatine=10:1), was supplied by Sigma-Aldrich (Steinheim, Germany).

Instrumentation

Mass spectrometric experiments were performed by electrospray ionization (ESI) coupled with a LTQ-FTICR (7 Tesla) mass spectrometer (Thermo Fisher Scientific, Bremen, Germany), equipped with a 20 W continuous CO_2-laser (Synrad, Mukilteo, WA, USA; 10.6 μm). For these experiments, standard solutions of GAs (1-5 mg/L) in 65:35 (v:v) acetonitrile/water (0.1% formic acid) were infused directly into the ESI interface via a syringe pump at a rate of 5 μL/min. The optimized experimental conditions of electrospray (ESI) ion source were: ESI needle voltage of +5 kV; capillary voltage +25V; temperature of the heated capillary of 300°C and the sheat gas (N_2) flow rate of 2 arbitrary units (a.u.). The instrument was externally calibrated with appropriate standards.

Mass spectrometric data were acquired in the positive ion mode while scanning *m/z* 50-1300 at rate of 2 scan/s.

Low-resolution MS^n (n=2-5) experiments were performed by collisional induced dissociation (CID). All analyses were achieved under automatic gain control (AGC) conditions using helium as the damping as well as the collision gas for MS^n experiments. On the CID-MS^n the most abundant ion was automatically selected as the precursor ion and fragmented up to the MS^5 stage, each successive most abundant product ion being selected again as the precursor ion for the next step. The isolation width was set to 2 *m/z* units. This method was applied at different energy ranging from 25% to 35% of arbitrary units (100% corresponding to a 35eV excitation voltage), as it ensures sufficiently intense product ion peaks and the precursor ion peak is reduced to less than 20% relative intensity.

For the high-resolution MS/MS experiments in infrared multiphoton dissociation (IRMPD), precursor ions were isolated in the linear ion trap and transferred into the ICR cell. The laser is mounted downstream of the FTICR cell, vertically on the back of the magnet. In the upper part of the electronics cabinet at the rear side of the instrument, a mirror unit deflects the laser beam into the magnet bore. The laser beam then enters the ICR cell through a ZnSe-coated lens, which is highly suited to IR radiation. The duration of laser irradiation was adapted to generate optimal fragmentation and varied between 100 and 350 ms. Typically, a medium IRMPD pulse, 290 ms at 100 % energy, was applied as photon irradiation for solasonine, solamargine and α-tomatine and a shorter irradiation time (200 ms) at a laser power of 100 % energy was applied at the dehydrotomatine.

Data were acquired and processed by Xcalibur software package (version 2.0 SR1 Thermo Fisher Scientific). Mass spectra were imported, elaborated and plotted by SigmaPlot 10.0 (Systat Software, Inc., London, UK). Precursor and product ion structures were drawn by ChemDraw Pro 14.0 (CambridgeSoft Corporation, Cambridge, MA, USA).

Results and Discussion

ESI(+)-FTICR MS/MS and ESI(+)-LIT-MS^n analysis of solasonine

Reported herein are results concerning the characterization of the spirosolane-type GA solasonine (Fig. 1a) by ESI(+)-LIT-FTICR MS and tandem mass spectrometry (MS/MS) performed by CID and IRMPD (Fig. 2). Solasonine, one of major glycoalkaloids found in eggplant, has an exact molecular mass of 883.49239 Da, while the ESI(+)-FTICR MS spectrum shows the proton adduct $[M+H]^+$ ion at accurate *m/z* 884.50085. The product ion at nominal *m/z* 866 (accurate *m/z* 866.48877), due to water loss, was observed in the both solasonine CID (MS^2), as most prominent product ion, and IRMPD MS/MS spectra (Fig. 2). The presence of signals at *m/z* 720 and 704 in the CID (MS^3) spectrum, suggests that these product ions result from fragmentation of dehydrated solasonine. Their accurate *m/z* values (720.43314 and 704.43799), obtained in the IRMPD spectrum, corroborate the nature of the sugar residue losses: the ion at *m/z* 720.43314 ($C_{39}H_{62}NO_{11}^+$) correspondes to the loss of a rhamnose mojety (146 Da, $Y_{2\beta}$-H_2O), one of the three sugars composing the aglycone-linked sugar chain, through glycosidic cleavage, and the ion at *m/z* 704.43799 ($C_{39}H_{62}NO_{10}^+$) results from the loss of a rhamnose and linker oxygen ($Z_{2\beta}$-H_2O) or from the loss of one glucose (162 Da, $Y_{2\alpha}$-H_2O). The nomenclature used in this paper for oligosaccharides fragmentation is based on that described by Domon and Costello [22]. Oligosaccharides show two types of common bond cleavages in MS/MS: glycosidic cleavages (B-, C-, Y-, Z-type) that break a bond between monosaccharides, and cross-ring cleavages (A- and X-type) that involve the breaking across carbohydrate rings [23]. Glycosidic cleavages provide information regarding monosaccharide composition while cross-ring cleavages are particularly helpful in determining linkage type [24].

In the CID MS^4 spectrum (i.e. fragmentation of the product ion at *m/z* 720, $Y_{2\beta}$-H_2O), the concomitant loss of both sugars and two water molecules produces the peak at *m/z* 378

(accurate value *m/z* 378.31611 in the IRMPD spectrum, Z_0-H_2O). From the same precursor ion, a galactose moiety loss (162 Da) generates the peak at *m/z* 558 (Y_1-H_2O, accurate *m/z* 558.37958 in the IRMPD spectrum), which is the aglycone with one glucose residue. The subsequent Z type ion at *m/z* 396.32633 (Z_0) is obtained by glucose loss (162 Da), corresponding to the aglycone solasodine deprived of a water molecule. The rise of the ion at *m/z* 396, Y_1-H_2O, is confirmed by the MS^5 CID analysis where the product ion at *m/z* 558 is isolated and fragmented. Otherwise, as shown in Fig. 3, the ion at exact *m/z* 396.32609 can be obtained directly from the aglycone after the loss of the trisaccharide moiety.

As shown in Fig.2, there are signals in the IRMPD spectrum that do not appear in the MS^n spectra, in particular the ions at accurate *m/z* 414.33698 (error 0.77 ppm), 271.20597 (error 1.21 ppm), 253.19527 (error 0.75 ppm), 157.10123 (error 0.02 ppm), 126.12775 (error 0.16 ppm) and 85.02842 (error 0.12 ppm). The peaks at *m/z* 414.33698, 271.20597, 253.19527 and 157.10123 are attributable to the aglycone formation and cleavage, and are due to the the solasodine product ion, to the E-ring moiety loss, to the consecutive elimination of water molecule and to the B-ring fragmentation, respectively. The peak at *m/z* 126.12775 represents the E-ring [14], while the peaks at accurate *m/z* 85.02842 (error 0.12 ppm), the most prominent ion in the IRMPD MS spectrum, derives from loss of one hexose residue. This last aspect, concerning the monosaccharide fragmentation, will be discussed in the next section. Interestingly, it should be noted that there is the chance to explore the low *m/z* range (hardly explored with the classical three-dimensional and two-dimensional ion traps) where it is possible to examine the presence of a signal at *m/z* 85.02842, which can certainly be considered a common product ion of GAs.

As shown in Fig. 2, both CID and IRMPD promote cleavage across the aglycon rings, resulting in highly diagnostic fragmentation patterns, but IRMPD shows a more rich spectrum in the low *m/z* range because ion-trap-based analyzers rely on the use of selective

frequency activation only for a certain relatively narrow interval of product ion masses around the precursor ion. Comparing the ESI-MS^n data with that of IRMPD MS/MS experiments (Table 1), the possible fragmentation patterns of solasonine can be proposed as shown in Fig. 3.

ESI(+)-FTICR MS and ESI(+)-MS/MS analysis of solamargine

The second major glycoalkaloid found in eggplant is known as solamargine (Fig. 1b). Here the characterization of solamargine (exact mass 867.49747 Da) performed by tandem mass spectrometry with both CID MS^n and FTICR-IRMPD MS/MS is discussed (Fig. 4). As mentioned above for solasonine, product ions from glycoside cleavage obtained by the two complementary fragmentation methods can provide useful information on the mass of aglycone and the sequence of oligosaccharide chains.

The product ion at *m/z* 850 $[M+H-H_2O]^+$ (accurate *m/z* 850.49511), generated by loss of one molecule of water from the $[M+H]^+$ ion, produces Y type product ions at *m/z* 704 ($Y_{2\beta}$, accurate *m/z* 704.43741) and 558 (Y_1, accurate *m/z* 558.38001), representing glycosidic cleavage by loss of one rhamnose residue (146 Da) and two rhamnose residues (146+ 146 Da), respectively (Fig. 4). The strong intensities of the two ions in the CID spectrum (data not shown) imply that these sugar residues are located at different termini of the sugar chains. A weak Y type ion at *m/z* 414 (Y_0, accurate *m/z* 414.33718) is produced by the simultaneous elimination of all three sugar chain moieties of solamargine (146+146+162 Da), forming the aglycone solasodine fragment, the same as obtained by MS/MS analysis of solasonine (Fig. 3a). There is no cross-ring ion detected at all. Since solasonine and solamargine differ from each other only in the sugar chain, the fragmentation behavior of solamargine aglycone is the same as seen for solasonine. In particular, the signals at *m/z* 396.32678, 378.31601, 271.20587, 253.19539, 157.10126 and 126.12775, due to the cleavage of steroidal aglycone

solasodine, are present in both solasonine and solamargine IRMPD MS/MS spectra. Based on the same consideration as used for solasonine, a proposed fragmentation pathway is shown in Fig. 5, obtained by interpretation of the IRMPD and CID spectra (Fig. 4). Also in this case, the CID MS/MS spectra are dominated by ions formed by breaking the weakest bonds, whereas they are devoid of "high-energy" ions detected only in the IRMPD spectrum that provide more complete structural information. The main IRMPD MS/MS product ions and the relative mass errors in ppm are summarised in Table 1.

The same features as discussed above for standard solutions of solamargine and solasonine were also observed in the mass spectra obtained from crude extracts of eggplants and Solanum nigrum berries (data not shown).

ESI(+)-FTICR MS and ESI(+)-MS/MS analysis of α-tomatine

The characterization of α-tomatine, the main glycoalkaloids found in tomato plants, by CID MS^n and IRMPD MS/MS analysis was performed (Fig, 6). Electrospray ionization of this molecule in positive ion mode yields the $[M + H]^+$ ion at accurate *m/z* 1034.55310. The fragmentation of this ion by CID (see Fig 6) generates three characteristic product ions which were of great importance for the determination of the sugar sequence of steroidal glycoalkaloids: the most intense at *m/z* 1016 (accurate *m/z* 1016.54224), indicating the loss of water molecule through a rearrangement process in the E ring; the ion at *m/z* 902 ($Y_{3\alpha}$, accurate *m/z* 902.50983), indicating the elimination of a xylose (132 Da), one of the four monosaccharide composing the sugar chain linked to the aglycone tomatidine; and the least abundant at *m/z* 740 (Y_2, accurate *m/z* 740.45776), due to the concomitant loss of xylose (132 Da) and glucose (162 Da). The ion at *m/z* 1016 can lose xylose (132 Da) or glucose (162 Da), generating the product ions at *m/z* 884 ($Y_{3\alpha}-H_2O$, accurate *m/z* 884.50073) and 854 ($Y_{3\beta}-H_2O$, accurate *m/z* 854.49033),

respectively. The competing losses of sugar units confirm that there are two different terminal residues in the lycotetraose, oligosaccharide chain, one a hexose unit and the other a pentose unit. From the loss of both xylose and glucose (132+162 Da), the product ion at *m/z* 722 (Y_2-H_2O, accurate *m/z* 722.44733) is obtained. An additional glucose loss generates the ion at *m/z* 560 (Y_1-H_2O, accurate *m/z* 560.39471) while the product ion at *m/z* 380 (Z_0-H_2O, accurate *m/z* 380.33099) is attributed to a loss of the remaining sugar, a galactose moiety (162 Da), producing the aglycone moiety deprived of two water molecules. The above MS^n data in positive ion mode confirm the number and sequence of sugar unit types (hexose or pentose) in the oligosaccharide chains, and the type of aglycon of GA.

Following another fragmentation pathway, the product ion at *m/z* 902.50983 produces an *m/z* 740.45776 ion by loss of a glucose molecule; the later generates a product ion at *m/z* 578.40491 by another glucose loss. In addition, by loss of a sugar moiety from the ion with *m/z* 740.45776, the characteristic tomatidine product ion (*m/z* 416.35236) is obtained [2]. After loss of the linked saccharides the favored fragmentation step of the aglycone is water elimination and double bond formation, resulting in a strong signal at *m/z* 398 (Z_0, accurate *m/z* 398.34180). The next fragmentation of the E-ring yields the ions at accurate *m/z* 126.12769 and *m/z* 273.22128, followed by the formation of the ion at *m/z* 255.21065 due to water loss from *m/z* 273 [2]. The ion at *m/z* 255 can then further dissociate to form the ion at *m/z* 157, attributable to cleavage of the B ring. Ions at accurate *m/z* 145.04905, 97.02837, 85.02837, 69.03346 would be formed by the cleavage of a hexose ring (see Fig. 10).

A proposed mechanism of solamargine fragmentation is shown in Fig. 7.

ESI(+)-FTICR MS and ESI(+)-MS/MS analysis of dehydrotomatine

Dehydrotomatine is another charactestic spirosolane-type glycoalkaloid found in tomato plants and it differs substantially from the α-tomatine by the presence of a double bond at position 5,6 in the B-ring of the steroidal skeleton. Moreover, its aglycone moiety, called tomatidenol, differs from solasodine in its E-ring stereochemistry. Figure 8 illustrates the characterization of dehydrotomatine by CID MS^n and IRMPD MS/MS. As shown in Fig. 8 (see inset), two MS^2 main product ions at *m/z* 900 and 576 were observed in the CID of the $[M+H]^+$ precursor ion at *m/z* 1032. These two ions arise from glycosidic bond cleavages of the glycosyl moieties of dehydrotomatine, i.e., lycotetraose, and such cleavages are useful for confirming the sugar species of the saccharide chain. The ion at *m/z* 900 corresponds to the loss of a pentose, so it was considered to be $[M\text{-}Xyl+H]^+$. The mass difference between the product ions at *m/z* 900 ($Y_{3\alpha,}$ accurate *m/z* 900.49530) and 576 ($Y_{1,}$ accurate *m/z* 576.38940) was 324 *m/z* units (162+162 Da), which suggested that the product ion at *m/z* 576 corresponds to the loss of two hexose units, Glu-Glu, from the $[M+H]^+$ ion of *m/z* 1032. As suggested by the CID spectra (see inset in Fig. 8), from the MS^4 of ion at *m/z* 576, the loss of galactose generates the typical product ion at *m/z* 414 (the aglycone moiety $Y_{0,}$ accurate *m/z* 414.33636) from which all the characteristic fragments of steroidal group arise in the same way as already seen for α-tomatine (accurate masses of ions: *m/z* 396.32574, 378.31519, 253.19487, 126.12763).

From the *m/z* 1014.52698 ion, a second fragmentation pathway, derived by the loss of xylose and glucose, can be suggested giving product ions at *m/z* 882 and 852 ($Y_{3\alpha}–H_2O$, accurate *m/z* 882.48444 and $Y_{3\beta}–H_2O$, accurate *m/z* 852.47394, respectively). These two ions also lead to the formation of a peak at *m/z* 558 ($Y_1–H_2O$, accurate *m/z* 558.37842) by the loss of the other two sugar rings, Glu-Glu or Xyl-Glu, respectively. Fragmentation of the ion at *m/z* 558 generates two other signals, at *m/z* 396 ($Z_{0,}$ accurate *m/z*

396.32574) and 378 (accurate *m/z* 378.31519), i.e. the aglycone moiety deprived of one and two water molecules, respectively.

A proposed mechanism of fragmentation is shown in Fig. 9, based on the interpretation of both IRMPD MS/MS and CID MS^n data.

Comparison of the SGAs fragmentation pathways

Under CID MS^n and IRMPD MS/MS, the $[M + H]^+$ ions of spirosolane GAs undergo extensive fragmentation, as summarized in Table 1 and Fig. 10. The characteristic fragmentations of sugar chain, which can provide the linkage information, were similarly present in both CID and IRMPD spectra, but the key advantage offered by IRMPD MS/MS in the FTICR cell is its accurate mass measurement, which provides the elemental composition of precursor and product ions with good accuracy. Moreover, multistage of CID (MS^3 or MS^4) is commonly needed to completely sequence the oligosaccharides, while IRMPD of the same compounds yielded the product ions corresponding to the loss of the first residue to the last residue during a single-stage tandem MS experiement (MS^2). Therefore, IRMPD is not only a fast and efficient MS/MS method but it can also potentially serve as a complementary technique to CID for the structural characterization of spirosolane GAs.

In summary, all the $[M + H]^+$ ions lose sugar rings (Fig. 10) generating ions typical for all GAs. The fragments can be assigned to Z and Y ions characteristic of the cleavage of glycosidic bonds, and these ions provide information on the monosaccharidic sequence in a straightforward way. Moreover, all spirosolane GAs under investigation preferentially lose water during fragmentation, producing a $[M+H-H_2O]^+$ as the base peak (Fig. 2b). The product ions, $[M+H-S_3]^+$, $[M+H-S_4]^+$, $[M+H-H_2O-S_3]^+$ and $[M+H-H_2O-S_4]^+$, represent glycosidic cleavages, involving separate neutral losses of the terminal residues from the branched sugar chain, but are also typical the formation of peaks due to the concomitant loss

of two or three saccharide units: $[M+H-S_3-S_4]^+$, $[M+H-H_2O-S_3-S_4]^+$, $[M+H- S_2-S_3-S_4]^+$, $[M+H-H_2O-S_2-S_3-S_4]^+$. This was followed by the characteristic fission of aglycone, in which all the sugar moieties were lost, to form diagnostic ions such as $[Agly+H]^+$, $[Agly+H-H_2O]^+$, $[Aglycone+H-143]^+$, $[Aglycone+H-143-H_2O]^+$ and so on. The characteristic $[Agly+H]^+$ ions at nominal *m/z* 414 and nominal *m/z* 416 correspond to aglycon solasodine for solamargine and solasonine, tomatidenol for dehydrotomatine, and tomatidine for α-tomatine, in agreement with their molecular masses.

From the fragmentation of steroidal group, the signals obtained are the same for all spirosolane GAs in this study, i.e. *m/z* 396, 378, 271, 253, except for α-tomatine that generates the same product ions but at 2 *m/z* units higher because of the absence of an unsaturation in the aglycone precursor (*m/z* 398, 380, 273 and 255). As can be seen in the IRMPD-FTICR mass spectra of all the spirosolane GAs under investigation (Figs. 2, 4, 6 and 8), some quite strong signals due to the cleavage of the sugar rings are present in all the spectra, one with the signal at nominal *m/z* 85, corresponding to $C_4H_5O_2^+$ (Fig. 10) [25], that dominates the spectra of solamargine and solasonine, probably because these two GAs have two hexose residues (Glu or Rha) at the termini of the sugar chain while α-tomatine and dehydrotomatine each have only one (Glu). The product ions at nominal *m/z* 97 and 69 [26], obtained from the hexose residues after loss of two water molecules and formation of the peaks at nominal *m/z* 129 and 145, were generated only from α-tomatine and dehydrotomatine, while the ion at *m/z* 57 is specific to solasonine and solamargine. In this regard, it is important to consider the role of the high-energy fragmentation of IRMPD and of high-resolution FTICRMS that allows us to explore the low *m/z* region of the spectrum and to provide reproducible and reliable information for spirosolane GAs structural characterization.

The list of all the product ion *m/z* values obtained by IRMPD MS/MS analysis of solasonine, solamargine, α-tomatine and deydrotomatine is shown in Table 1**.** A scheme describing the major fragments found in MS/MS SGAs analysis is displayed in Fig. 10.

Some of these fragments correspond to hydrolysis products (metabolites) of GAs that are found in plant tissues and are formed during normal digestion and metabolism of the parent GAs after consumption. In effect, hydrolytic removal of sugar groups from the trisaccharide or tetrasaccharide sugar chain results in the formation of β-, γ- and δ derivatives, corresponding to aglycone with three, two, and one sugar, respectively [27].

Accurate detection of GAs and their hydrolysis products is of great interest because they play a major role in disease resistance in Solanaceae plants and may be biologically active in animals and humans. Previous studies have shown that these compounds are potent inhibitors of human colon and liver carcinoma cells [28] and exhibit antibiotic activities against bacteria, fungi, and viruses [29, 30]. Their relative potency is influenced by the chemical structure of the carbohydrate, the number of carbohydrate groups attached to the 3-OH position of the aglycones, and the structure of the aglycone; generally, the activities of the hydrolysis products are less than those of the parent GAs at the lower concentrations.

Conclusions

In this study, the structural characterization of major SGAs was performed using the fragmentation techniques CID MS^n and IRMPD MS/MS. Our results show that CID and IRMPD provide complementary structural information for SGAs characterization. Thanks to the multistage CID it was possible to understand the exact fragmentation pathway and thanks to the high resolution of IRMPD-FTICR the exact structures of product ions were obtained. All of the precursors and product ions were determined with errors of less than 2 ppm. MS^n (n = 2–5) studies on SGAs using LIT MS generated data showing the sequence of cleavages of the different sugar moieties. Moreover, the fragmentation of the aglycone led to the most abundant product ions, generated from cleavages at the B-ring and E-ring regions of this steroidal group.

Finally, because CID and IRMPD can be performed with the same instrument, the analysis of glycoalkaloids can be streamlined and performed without extensive sample handling and dispersal.

Table 1. Characteristic ions observed in the IRMPD MS/MS spectra of spirosolane GAs

Characteristic ions	**Main IRMPD MS/MS product ions (accurate *m/z*) [a] and mass error (ppm) [b]**	
	Solasonine	**Solamargine**
$[M+H]^+$	884.50084 (0.71)	868.50557 (0.31)
$[M-H_2O+H]^+$	866.48877 (-1.02)	850.49511 (0.45)
$[M-Rha+H]^+$	720.43153 (-0.29)	-
$[M-Rha-O+H]^+$	704.43799 (0.72)	704.43741 (0.84)
$[M-Hex^*-Rha-H_2O+H]^+$	558.37958 (1.20)	558.38001 (1.97)
$[M-Hex^*-Rha-Glc+H]^+$	414.33698 (0.77)	414.33718 (1.26)
$[M-Hex^*-Rha-Glc-H_2O+H]^+$	396.32633 (0.60)	396.32678 (1.74)
$[M-Hex^*-Rha-Glc-2H_2O+H]^+$	378.31611 (1.53)	378.31601 (1.27)
$[C_{19}H_{26}O+H]^+$	271.20597 (1.21)	271.20587 (0.85)
$[C_{19}H_{24}+H]^+$	253.19527 (0.75)	253.19539 (1.22)
$[C_{13}H_{14}+H]^+$	171.11706 (1.34)	-
$[C_{12}H_{12}+H]^+$	157.10123 (0.02)	157.10126 (0.51)
$[C_6H_8O_3+H]^+$	129.05475 (1.01)	129.05466 (0.31)
$[C_8H_{15}N+H]^+$	126.12775 (0.16)	126.12775 (0.16)
$[C_4H_4O_2+H]^+$	85.02842 (0.12)	85.02842 (0.12)
$[C_4H_6O+H]^+$	71.04915 (0.14)	71.04911 (-0.42)
$[C_3H_4O+H]^+$	57.03348 (-0.17)	57.03347 (-0.35)
	Tomatine	**Dehydrotomatine**
$[M+H]^+$	1034.5531 (0.07)	1032.53687 (-0.49)
$[M-H_2O+H]^+$	1016.54224 (-0.23)	1014.52682 (-0.07)
$[M-Xyl+H]^+$	902.50983 (-1.05)	900.49530 (0.19)
$[M-Xyl-H_2O+H]^+$	884.50073 (0.59)	882.48444 (-0.14)
$[M-Glc+H]^+$	854.49023 (0.68)	852.47394 (-0.07)
$[M-Glc-Xyl+H]^+$	740.45776 (-0.26)	-
$[M-Glc-Xyl-H_2O+H]^+$	722.44733 (-0.08)	-

$[M-2Glc-Xyl+H]^+$	578.40491 (-0.38)	576.38940 (-0.14)
$[M-2Glc-Xyl-H_2O+H]^+$	560.39471 (0.27)	558.37842 (-0.88)
$[M-Gal-2Glc-Xyl+H]^+$	416.35236 (0.12)	414.33636 (-0.72)
$[M-Gal-2Glc-Xyl-H_2O+H]^+$	398.3418 (0.15)	396.32574 (-0.88)
$[M-Gal-2Glc-Xyl-2H_2O+H]^+$	380.33099 (-0.50)	378.31553 (0.90)
$[C_{19}H_{28}O+H]^+$	273.22128 (-0.04)	-
$[C_{19}H_{24}+H]^+$	-	253.19487 (-0.83)
$[C_{19}H_{26}+H]^+$	255.21065 (-0.31)	-
$[C_{13}H_{15}+H]^+$	173.13243 (-0.29)	-
$[C_{12}H_{12}+H]^+$	-	157.10109 (-0.57)
$[C_{12}H_{14}+H]^+$	159.11678 (-0.31)	-
$[C_6H_8O_4+H]^+$	145.04948 (-0.41)	145.04945 (-0.62)
$[C_8H_{15}N+H]^+$	126.12769 (-0.32)	126.12763 (-0.79)
$[C_5H_4O_2+H]^+$	97.02837 (-0.41)	97.02833 (-0.82)
$[C_4H_4O_2+H]^+$	85.02837 (-0.47)	85.02835 (-0.70)
$[C_4H_4O+H]^+$	69.03346 (-0.43)	-

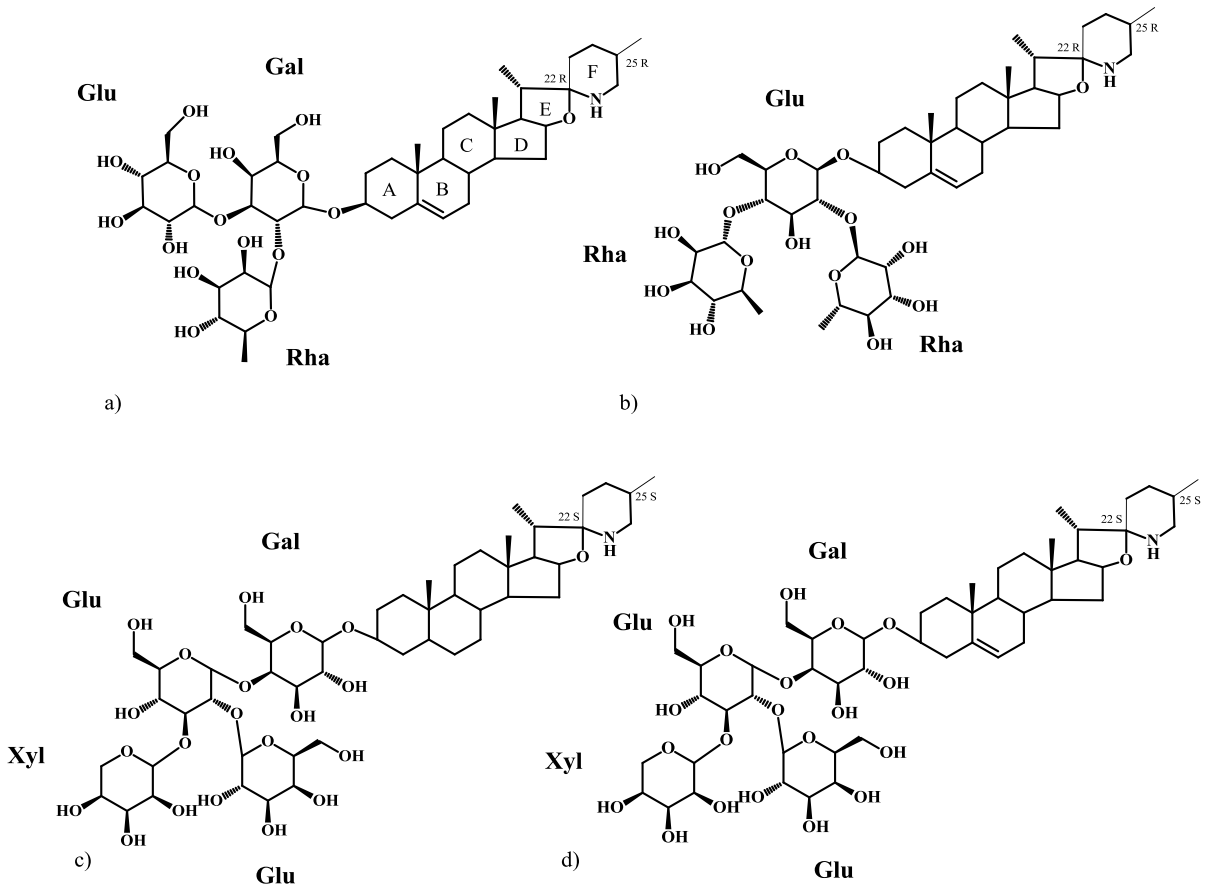

Figure 1. (a) solasonine; (b) solamargine; (c) α-tomatine; (d) dehydrotomatine structures.

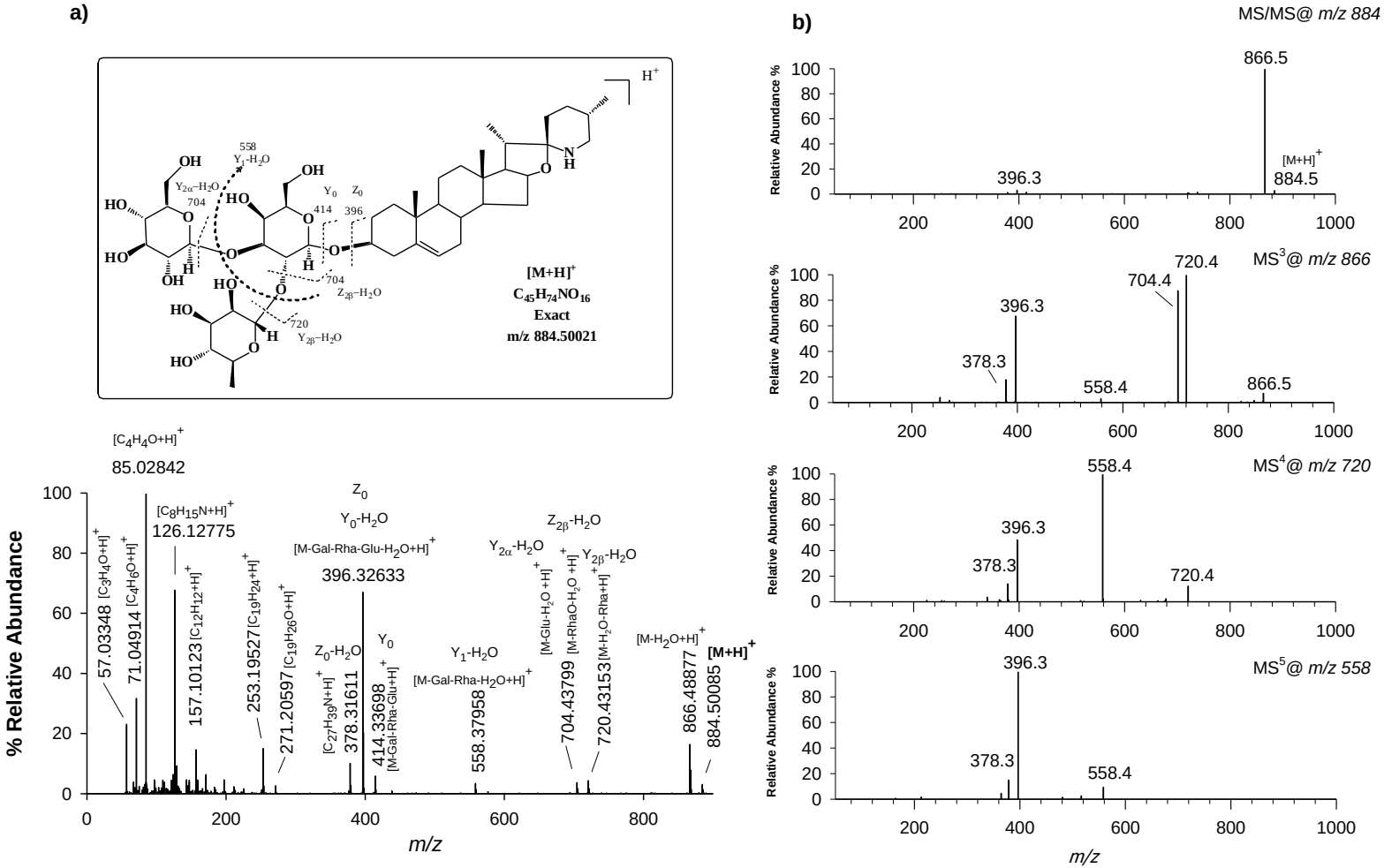

Fig. 2 Mass spectra of solasonine: a) FT-ICR IRMPD MS spectrum, the $[M+H]^+$ precursor ion was photonirradiated for 290 ms at 100% laser power; b) CID MS spectra, relative collision energies ranging from 25% to 35% were applied.

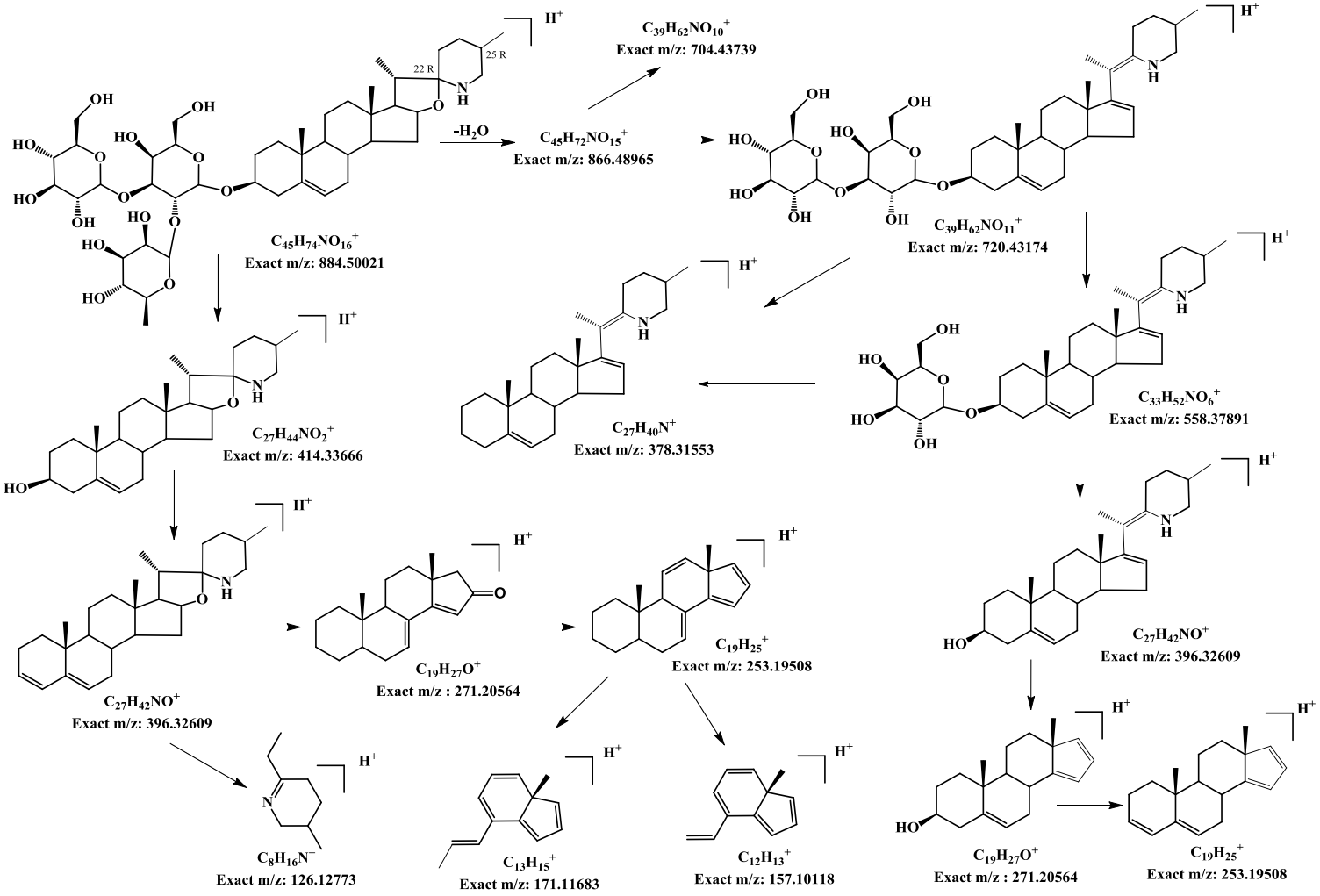

Fig. 3. Proposed fragmentation pathway for solasonine, based on CID MS^n and IRMPD MS/MS spectra

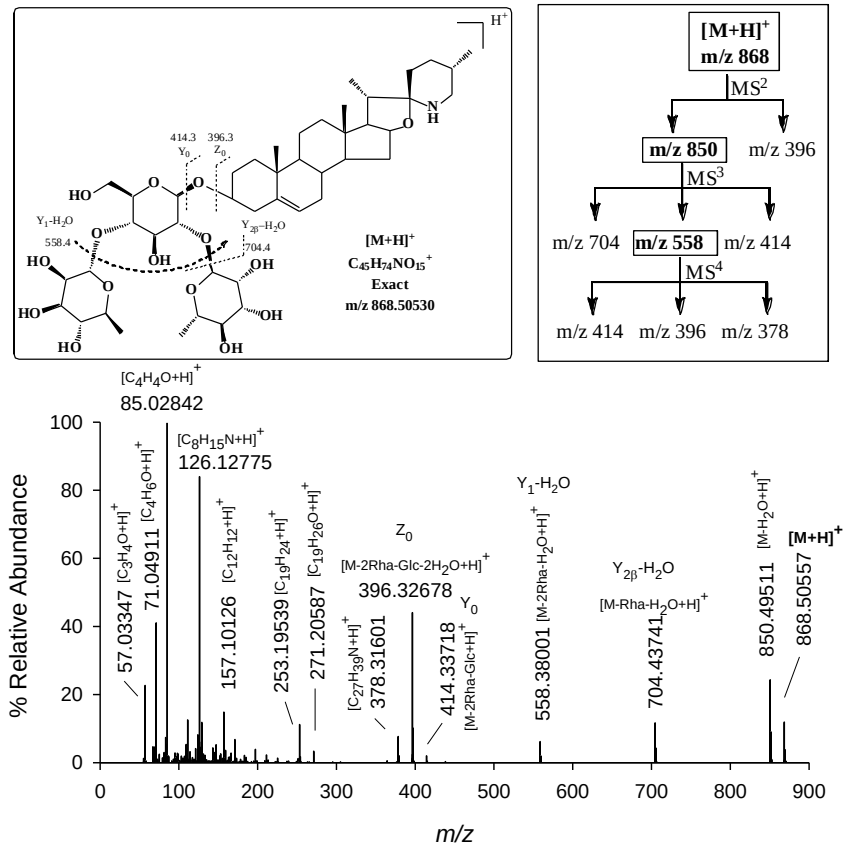

Fig 4. FT-ICR IRMPD MS spectrum of solamargine; the $[M+H]^+$ precursor ion was photonirradiated for 290 ms at 100% laser power. Inset shows the CID MS^n fragmentation.

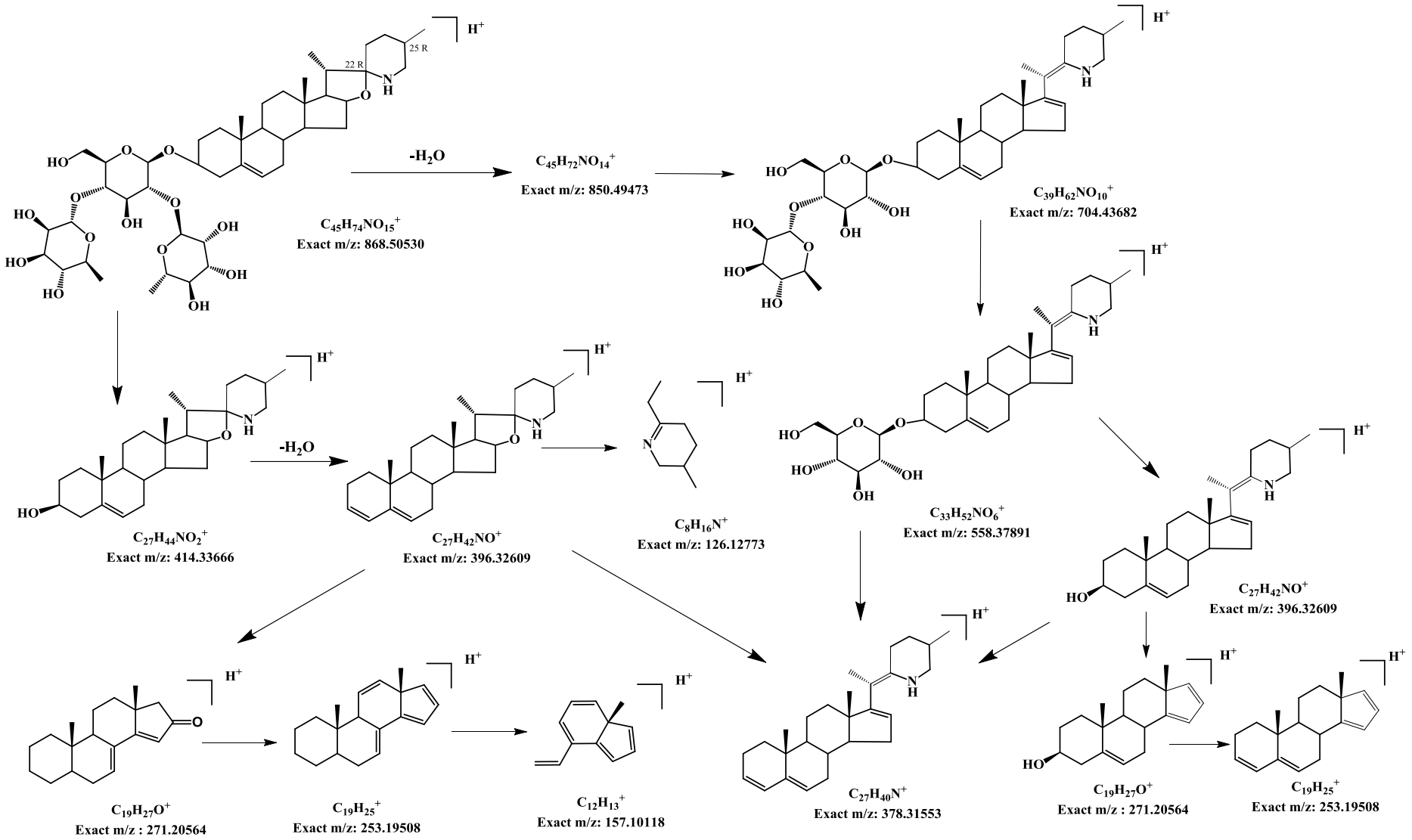

Fig. 5. Proposed fragmentation pathway for solamargine, based on CID MS^n and IRMPD MS/MS spectra

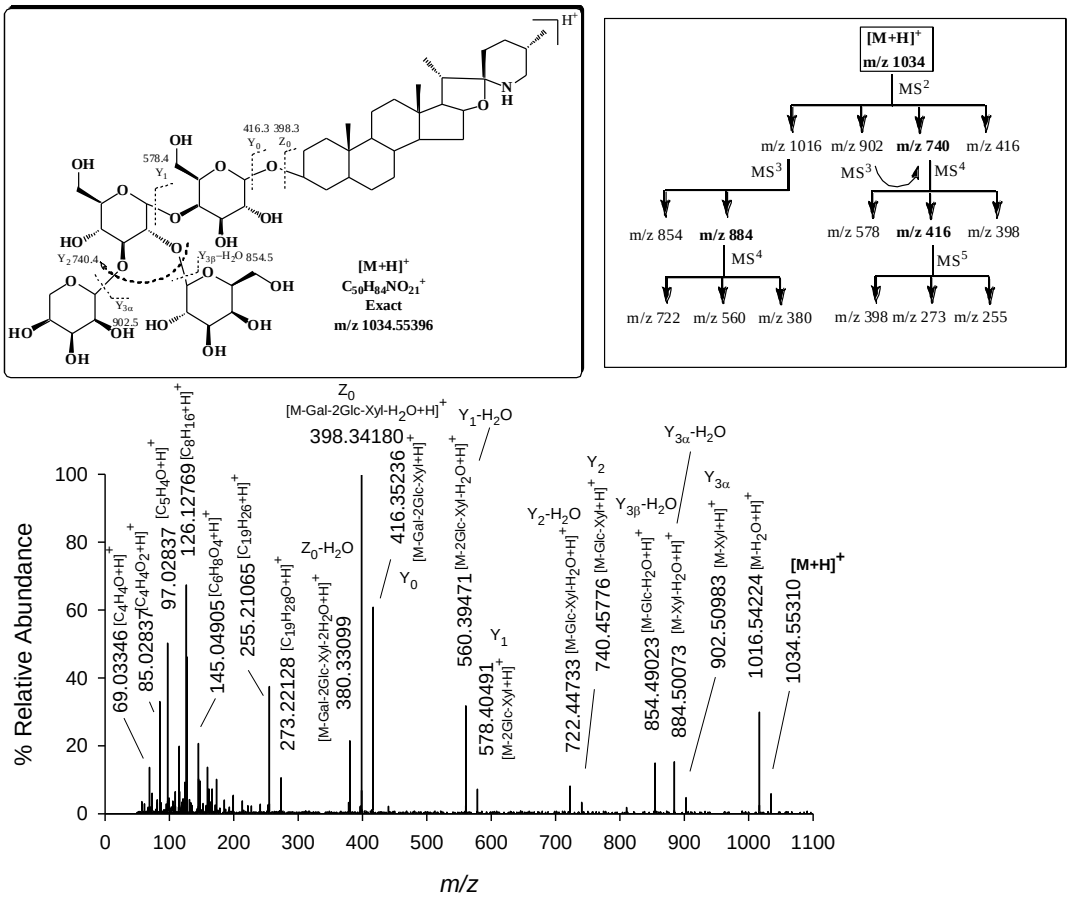

Fig 6. FT-ICR IRMPD MS spectrum of α-tomatine; the $[M+H]^+$ precursor ion was photonirradiated for 290 ms at 100% laser power. Inset shows the CID MS^n fragmentation.

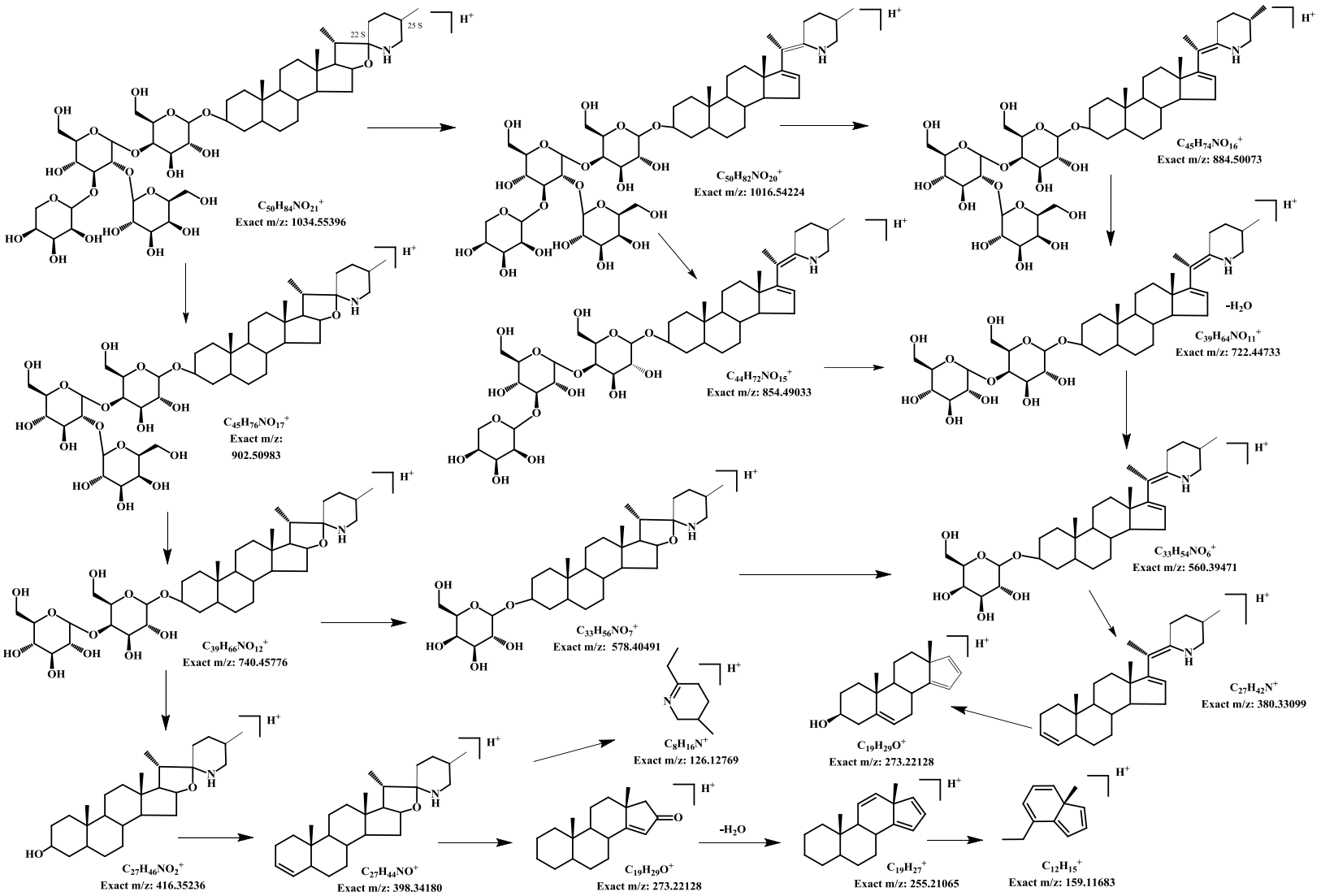

Fig. 7. Proposed fragmentation pathway for α-tomatine. Characterization of the α–tomatine by CID MS^n and IRMPD MS/MS spectra.

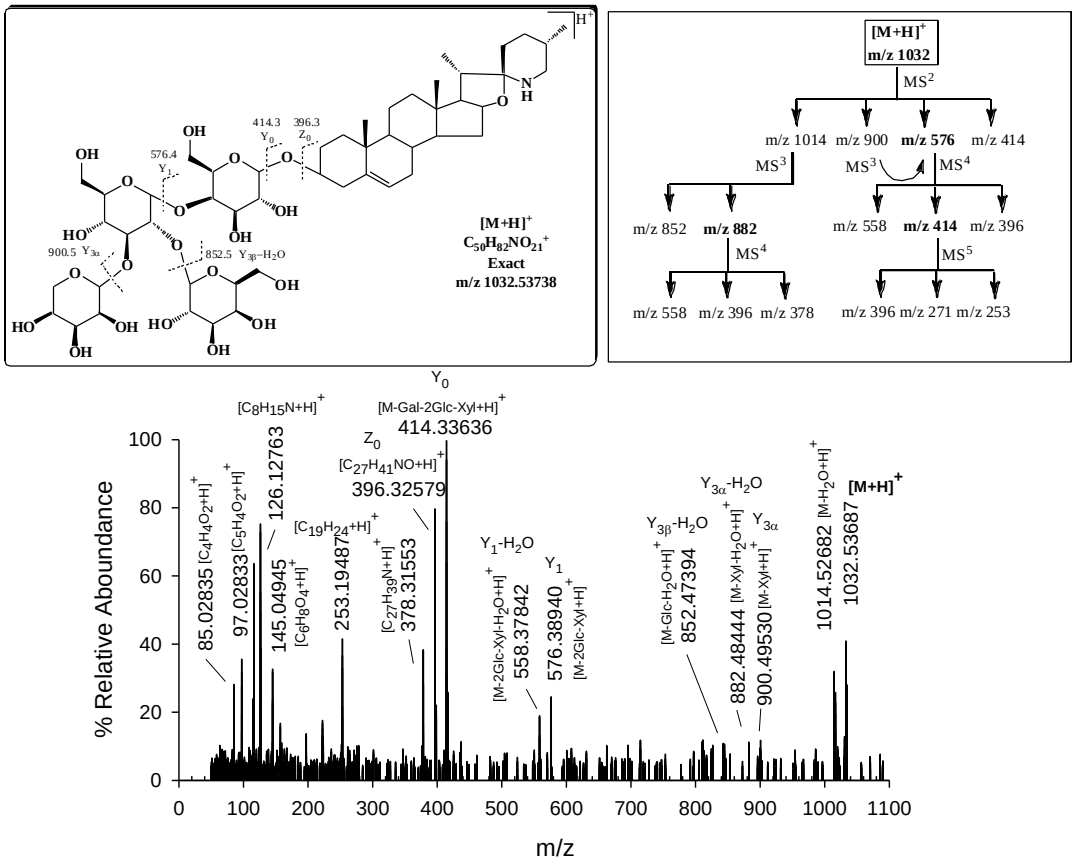

Fig. 8. FT-ICR IRMPD MS spectrum of dehydrotomatine; the $[M+H]^+$ precursor ion was photonirradiated for 200 ms at 100% laser power

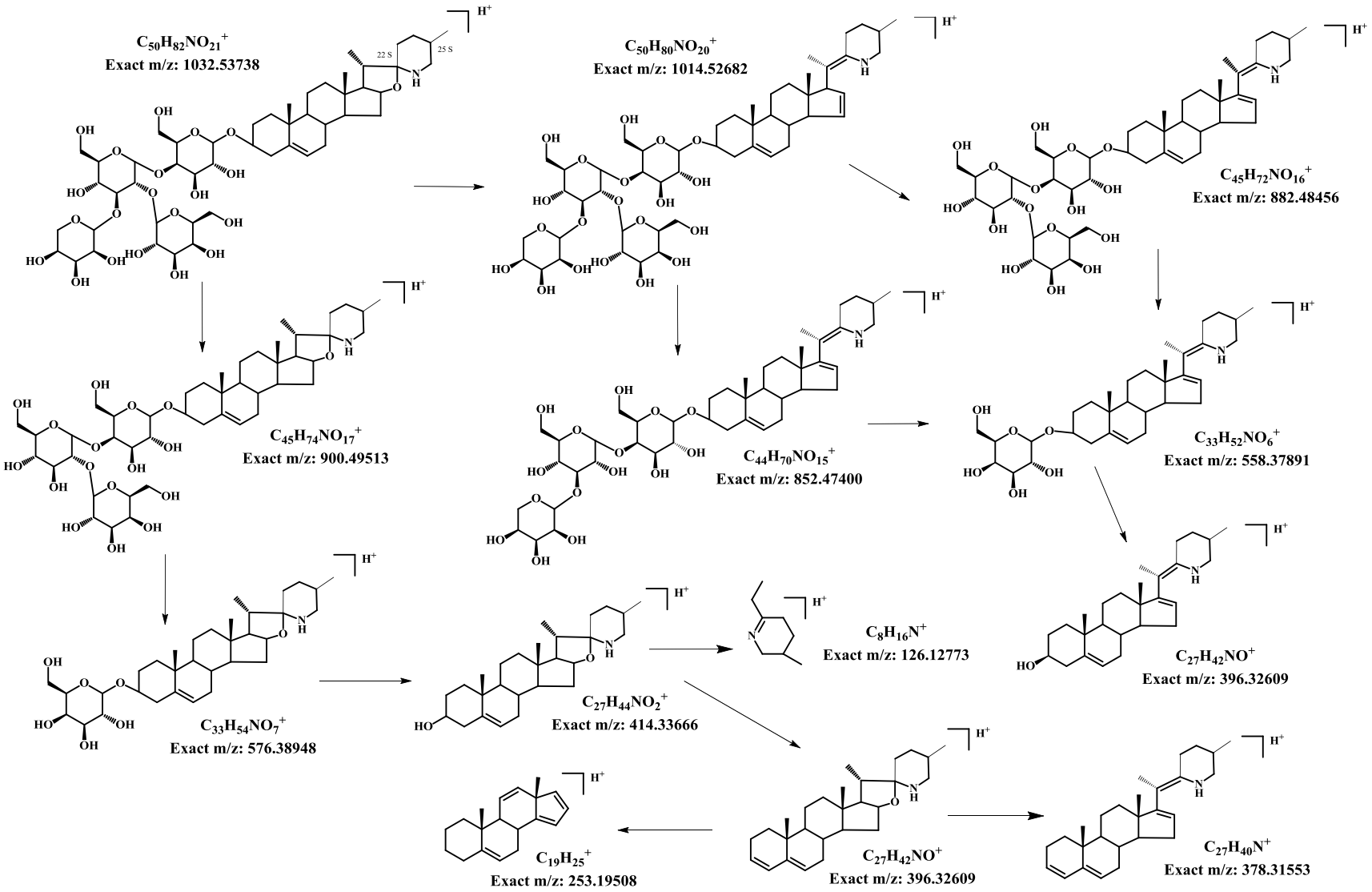

Fig. 9. Proposed fragmentation pathway for dehydrotomatine. Characterization of the dehydrotomatine by CID MS^n and IRMPD MS/MS spectra.

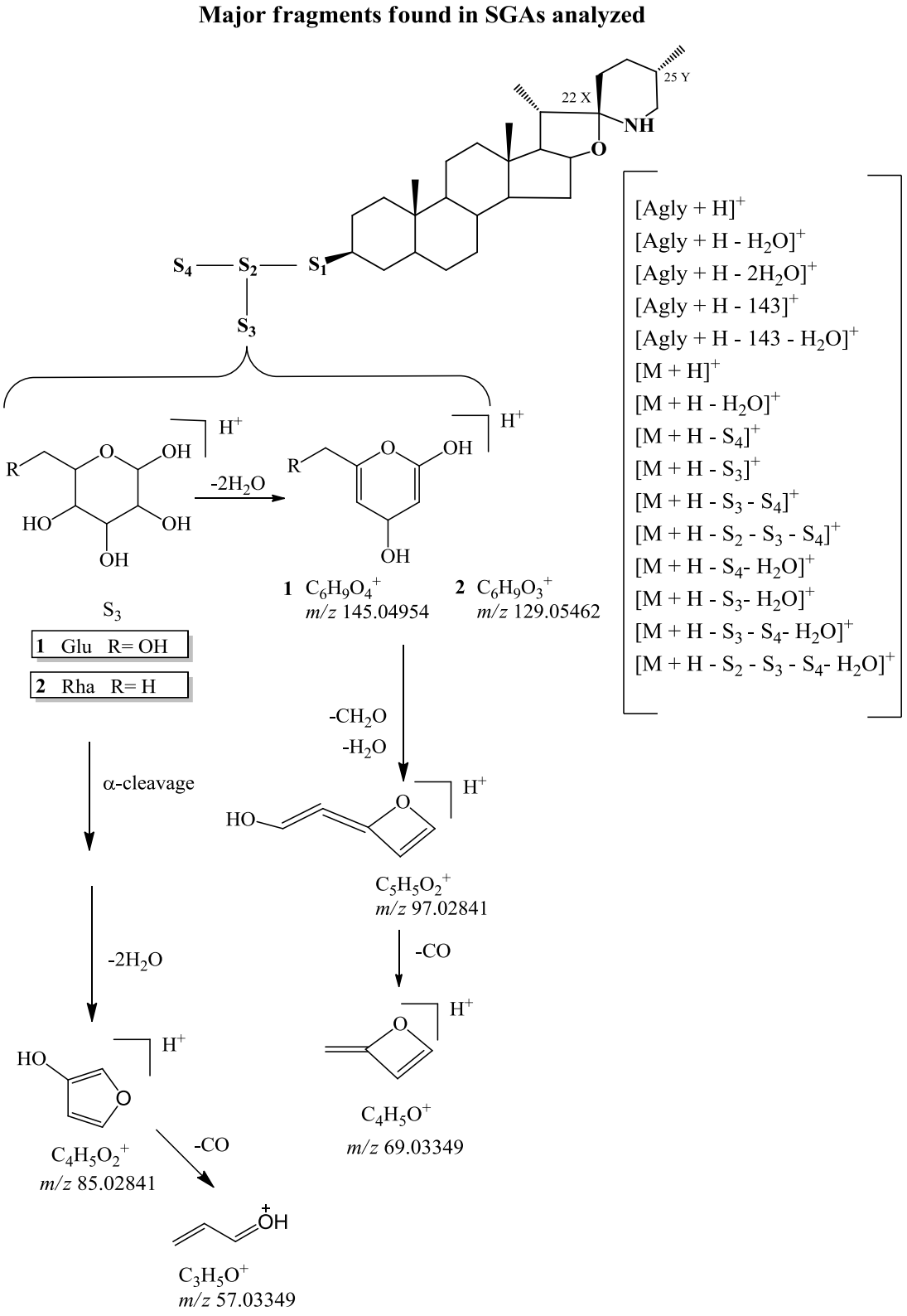

Fig. 10. Typical tandem mass spectrometry fragmentation behavior of spirosolane GAs and proposed fragmentation pathway for terminal hexose residue. Symbols S1 –S4 indicate the different sugar rings.

REFERENCES

[1] S. B. Wu, R. S.Meyer, B. D. Whitaker, A. Litt, E. J. Kennelly. A new liquid chromatography–mass spectrometry-based strategy to integrate chemistry, morphology, and evolution of eggplant (Solanum) species. *J. Chromatogr. A* **2013**, *1314*, 154.

[2] T. R. Cataldi, F. Lelario, S. A. Bufo. Analysis of tomato glycoalkaloids by liquid chromatography coupled with electrospray ionization tandem mass spectrometry. *Rapid. Commun. Mass Spectrom.* **2005**, *19*, 3103.

[3] P. Marciniak, Z. Adamski, P. Bednarz, M. Slocinska, K. Ziemnicki, F. Lelario, L. Scrano, S. A. Bufo. Cardioinhibitory properties of potato glycoalkaloids in beetles. *Bulletin of environmental contamination and toxicology* **2010**, *84*, 153.

[4]S. Chowański, Z. Adamski, P. Marciniak, G. Rosiński, E. Büyükgüzel, K. Büyükgüzel, P. Falabella , L. Scrano , E. Ventrella, F. Lelario, S. A. Bufo. A review of bioinsecticidal activity of Solanaceae alkaloids. *Toxins* **2016**, *8*, 60.

[5] T. T. Mensinga, A. J. Sips, C. J. Rompelberg, K. van Twillert, J. Meulenbelt, H. J. van den Top, H. P. van Egmond. Potato glycoalkaloids and adverse effects in humans: an ascending dose study. *Regul. Toxicol. Pharmacol.* **2005**, *41*, 66.

[6] J. T. Blankemeyer, M. L. McWilliams, J. R. Rayburn, M. Weissenberg, M. Friedman. Developmental toxicology of solamargine and solasonine glycoalkaloids in frog embryos. *Food Chem. Toxicol*. **1998**, *36*, 383.

[7] I. Ginzberg, J. G. Tokuhisa, R. E. Veilleux. Potato Steroidal Glycoalkaloids: Biosynthesis and Genetic Manipulation. *Potato Research* **2009**, *52*, 1.

[8] M. Itkin, I. Rogachev, N. Alkan, T. Rosenberg, S. Malitsky, L. Masini, S. Meir, Y. Iijima, K. Aoki, R. de Vos, D. Prusky, S. Burdman, J. Beekwilder, A. Aharon. GLYCOALKALOID

METABOLISM1 Is Required for Steroidal Alkaloid Glycosylation and Prevention of Phytotoxicity in Tomato. *Plant Cell.* **2011**, *23*, 4507.

[9] S. Chen, P. J. Derrick, F. A. Mellon, K. R. Price. Analysis of Glycoalkaloids from Potato Shoots and Tomatoes by Four-Sector Tandem Mass Spectrometry with Scanning-Array Detection: Comparison of Positive Ion and Negative Ion Methods. *Anal. Biochem*. **1994**, *218*, 157.

[10] H. Ono, D. Kozuka, Y. Chiba, A. Horigane, K. Isshiki. Structure and cytotoxicity of dehydrotomatine, a minor component of tomato glycoalkaloids. *J. Agric. Food Chem.* **1997**, *45*, 3743.

[11] M. Claeys, H. Van den Heuvel, S. Chen, P. J. Derrick, F. A. Mellon, K. R. Price. Comparison of high- and low-energy collision-induced dissociation tandem mass spectrometry in the analysis of glycoalkaloids and their aglycons. *J. Am. Soc. Mass Spectrom*. **1996**, *7*, 173.

[12] B. Zywicki, G. Catchpole, J. Draper, O. Fiehn. Comparison of rapid liquid chromatography-electrospray ionization-tandem mass spectrometry methods for determination of glycoalkaloids in transgenic field-grown potatoes. *Anal. Biochem.* **2005**, *336*, 178.

[13] M.G. Cahill, G. Caprioli, S. Vittori, K. J. James. Elucidation of the mass fragmentation pathways of potato glycoalkaloids and aglycons using Orbitrapmass spectrometry. *J. Mass Spectrom.* **2010**, *45*, 1019.

[14] G. Caprioli, M. G. Cahill, K. J. James. Mass fragmentation studies of α-tomatine and validation of a liquid chromatography LTQ orbitrap mass spectrometry method for its quantification in Tomatoes. *Food Anal. Methods* **2014**, *7*, 1565.

[15] J. J. Jared, L. K. Murungi, J.Wesonga, B. Torto. Steroidal glycoalkaloids: chemical defence of edible African nightshades against the tomato red spider mite, Tetranychus evansi (Acari: Tetranychidae). Pest management science. *Pest Manag. Sci.* **2015**, *72*, 828.

[16] F. Lelario, G. Bianco, S. A. Bufo, T. R. Cataldi. Establishing the occurrence of major and minor glucosinolates in Brassicaceae by LC–ESI-hybrid linear ion-trap and Fourier-transform ion cyclotron resonance mass spectrometry. *Phytochem.* **2012**, *73*, 74.

[17] N. C. Polfer. Infrared multiple photon dissociation spectroscopy of trapped ions. *Chem. Soc. Rev.* **2011**, *40*, 2211.

[18] S. A. Raspopov, A. El-Faramawy, B. A. Thomson, K. M. Siu. Infrared multiphoton dissociation in quadrupole time-of-flight mass spectrometry: top-down characterization of proteins. *Anal. Chem.* **2006**, *78*, 4572.

[19] J. A. Madsen, J. S. Brodbelt. Comparison of Infrared Multiphoton Dissociation and Collision-Induced Dissociation of Supercharged Peptides in Ion Traps. *J. Am. Soc. Mass Spectrom.* **2009**, *20*, 349.

[20] G. Bianco, C. Labella, A. Pepe, T. R. I. Cataldi Scrambling of autoinducing precursor peptides investigated by infrared multiphoton dissociation with electrospray ionization and Fourier transform ion cyclotron resonance mass spectrometry. *Anal. Bioanal. Chem.* **2013**, *405*, 1721.

[21] G. Bianco, F. Lelario, F. G. Battista, S. A. Bufo, T. R. Cataldi. Identification of glucosinolates in capers by LC-ESI-hybrid linear ion trap with Fourier transform ion cyclotron resonance mass spectrometry (LC-ESI-LTQ-FTICR MS) and infrared multiphoton dissociation. *J. Mass Spectrom.* **2012**, *47*, 1160.

[22] B. Domon, C. E. Costello. A systematic nomenclature for carbohydrate fragmentations in FAB-MS MS spectra of glycoconjugates. *Glycoconj. J.* **1988**, *5*, 397.

[23] W. Zhou, K. Håkansson. Structural characterization of carbohydrates by fourier transform tandem mass spectrometry. *Curr. Proteomics* **2011**, *8*, 297.

[24] J. T. Adamson, K. Håkansson. Electron Detachment Dissociation of Neutral and Sialylated Oligosaccharides. *J. Am. Soc. Mass Spectrom*. **2007**, *18*, 2162

[25] E. S. Berman, K. S. Kulp, M. G. Knize, L. Wu, E. J. Nelson, D. O. Nelson, K. J. Wu. Distinguishing monosaccharide stereo- and structural isomers with TOF-SIMS and multivariate statistical analysis. *Anal Chem.* **2006**, *78*, 6497.

[26] V. F. Taylor, R. E. March, H. P. Longerich, C. J. Stadey. A mass spectrometric study of glucose, sucrose, and fructose using an inductively coupled plasma and electrospray ionization. *Int. J. Mass Spectrom*. **2005**, *243*, 71.

[27] M. Friedman. Tomato glycoalkaloids: role in the plant and in the diet. *J. Agric. Food Chem*. **2002,** *50*, 5751.

[28] K. R. Lee, N. Kozukue, J. S. Han, J. H. Park, E. Y. Chang, E. J., Baek, J. S. Chang, M. Friedman, M. Glycoalkaloids and metabolites inhibit the growth of human colon (HT29) and liver (HepG2) cancer cells. *J. Agric. Food Chem.* **2004**, *52*, 2832.

[29] A. M. Fewell, J. G. Roddick, M. Weissenberg. Interactions between the glycoalkaloids solasonine and solamargine in relation to inhibition of fungal growth. *Phytochem.* **1994**, *37*, 1007.

[30] H. V. Thorne, G. F. Clarke, R. Skuce. The inactivation of herpes simplex virus by some Solanaceae glycoalkaloids. *AntiViral Res*.**1985**, *5*, 335.